

Carbon Dioxide in Ionic Liquid Microemulsions**

Jianling Zhang,* Buxing Han,* Jianshen Li, Yueju Zhao, and Guanying Yang

A microemulsion is a thermodynamically stable dispersion of two immiscible fluids stabilized by surfactants. The hydrophilic head groups of the surfactants point to the polar phase, while the hydrophobic tails extend into an apolar phase. Owing to the capacity to host a variety of polar and nonpolar species simultaneously, microemulsions have been widely applied in protein delivery,^[1] drug release,^[2] catalysis,^[3] and nanomaterials synthesis.^[4] In general, the organic solvent (oil) and water are used as the two immiscible fluids in the formation of microemulsions.

In recent years, especially with the development of green chemistry, supercritical CO₂ (SC CO₂) and ionic liquids (ILs), which are usually regarded as green solvents, have attracted much attention. In comparison with the conventional solvents (usually water and organic solvents), these green solvents have some unique properties. For example, SC CO₂ is readily available, inexpensive, nontoxic, nonflammable, and has moderate critical temperature and pressure. Most importantly, the physical properties of SC CO₂ can be adjusted by the pressure and temperature continuously.^[5] Furthermore, CO₂ can be easily recaptured and recycled after utilization. ILs are an interesting class of tunable and designable solvents with essentially zero volatility, wide electrochemical window, nonflammability, high thermal stability, and wide liquid range.^[6] Such unique properties confer SC CO₂ and ILs great potential of applications in chemistry and chemical engineering.

The formation of microemulsions with SC CO₂ or IL is very attractive owing to their unusual solvent properties. Up to now, various kinds of microemulsions containing SC CO₂ or IL have been prepared, including water-in-SC CO₂^[7] and CO₂-in-water microemulsions,^[8] IL-in-oil and oil-in-IL microemulsions,^[9] IL-in-water and water-in-IL microemulsions,^[10] IL-in-IL microemulsion,^[11] and IL-in-SC CO₂ microemulsions.^[12]

The creation of microemulsions with IL as the continuous phase and CO₂ as the dispersed phase is very interesting and

has not yet been reported. Herein, we demonstrate the first work for the formation of a CO₂-in-IL microemulsion. This novel microemulsion has many advantages. For example, the size of the dispersed CO₂ droplet can be tuned by the pressure of CO₂; the properties of the continuous phase can also be tuned by the kind of ILs because of the tunable and designable features of ILs. These special properties give CO₂-in-IL microemulsion various applications such as in material synthesis, chemical reactions, and extraction.

It is well known that the amphiphilic surfactant can self-assemble in ILs to form different aggregates such as micelles, vesicles, or liquid crystals.^[13] In this work, the aggregation behavior of surfactant *N*-ethyl perfluorooctylsulfonamide (C₂H₅NHSO₂C₈F₁₇, *N*-EtFOSA) in 1,1,3,3-tetramethylguanidium acetate (TMGA) ([*N*-EtFOSA] = 3.0 wt %) was characterized by freeze fracture electron microscopy (FFEM). As shown in Figure 1, *N*-EtFOSA molecules aggregated into spherical micelles in TMGA with an average diameter of 10–20 nm.

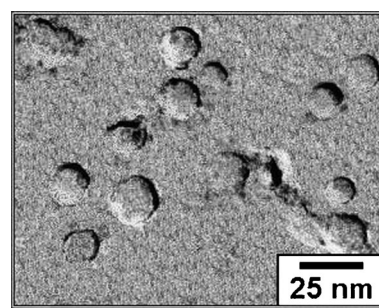


Figure 1. Freeze fracture electron microscopy image of *N*-EtFOSA/TMGA solution ([*N*-EtFOSA] = 3.0 wt %).

The phase behavior of the *N*-EtFOSA/TMGA solution ([*N*-EtFOSA] = 3.0 wt %) in the presence of CO₂ was observed at 293.2 K in the pressure range of 0–10 MPa. The compressed CO₂ was well solubilized in the surfactant solution and expanded the solution. As the pressure was higher than 5.7 MPa, the saturated vapor pressure of CO₂ at 293.2 K, an upper liquid CO₂ phase appeared and its volume increased with the increasing pressure. The bottom solution was clear and thermodynamically stable at all the pressures of CO₂. The schematic demonstration of phase behavior of the *N*-EtFOSA/TMGA solution at different CO₂ pressures is presented in Figure S1 in the Supporting Information.

The solubilities of CO₂ in *N*-EtFOSA/TMGA solution ([*N*-EtFOSA] = 3.0 wt %) and in pure TMGA were determined at 293.2 K and are shown in Figure 2. At low pressures, the CO₂ solubility in *N*-EtFOSA/TMGA solution is slightly higher than that in pure TMGA. As the pressure approaches

[*] Dr. J. Zhang, Prof. B. Han, J. Li, Dr. Y. Zhao, G. Yang
Beijing National Laboratory for Molecular Sciences, CAS Key
Laboratory of Colloid and Interface and Thermodynamics, Institute
of Chemistry, Chinese Academy of Sciences (China)
E-mail: zhangjl@iccas.ac.cn
hanbx@iccas.ac.cn

[**] We thank the National Natural Science Foundation of China (20873164, 21073207), the K. C. Wong Education Foundation (Hong Kong), the Ministry of Science and Technology of China (2009CB930802), the Chinese Academy of Sciences (KJCX2.YW.H16). We are also grateful to Prof. Zhonghua Wu from Beijing Synchrotron Radiation Facility (BSRF) for his help on the experiment of small-angle X-ray scattering.

Supporting information for this article is available on the WWW under <http://dx.doi.org/10.1002/anie.201103956>.

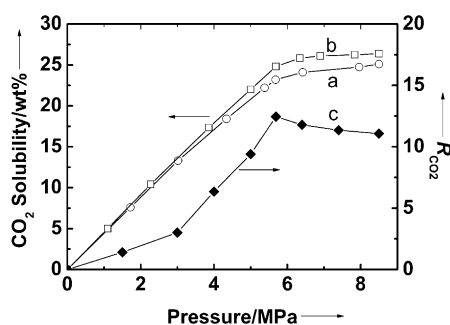


Figure 2. Solubility of CO₂ in a) pure TMGA and b) *N*-EtFOSA/TMGA solution ([*N*-EtFOSA] = 3.0 wt%); c) molar ratio of CO₂ in micelles to surfactant (R_{CO_2}) at various pressures.

5.7 MPa, the enhancement of the CO₂ solubility by adding *N*-EtFOSA is most remarkable. Then, the CO₂ solubilities in both *N*-EtFOSA/TMGA solution and pure TMGA are increased slightly with the pressure. The capability of the micelles to solubilize CO₂ is responsible for the enhanced CO₂ solubility.^[8a] The amount of CO₂ solubilized in the micelles, characterized by the molar ratio of CO₂ in micelles to surfactant (R_{CO_2}), was calculated by subtracting the CO₂ solubility in pure IL from the total amount of CO₂ in the solution, assuming that the IL was saturated by CO₂. As shown in Figure 2, R_{CO_2} increases with pressure and reaches a maximum at 5.7 MPa. At pressures higher than 5.7 MPa, R_{CO_2} decreases slightly with increasing pressure, which is similar to the result observed for the CO₂-in-water microemulsion.^[8a] One of the main reasons for this decrease may be that above 5.7 MPa the stability of the micelles decreases with increasing CO₂ pressure because the concentration of CO₂ in the continuous phase increases. The R_{CO_2} value reaches a maximum of 12.5 at 5.7 MPa, which is higher than that of CO₂-in-water microemulsion (6 at 298.2 K and 8 at temperatures from 308.2 K to 348.2 K).^[8a] Such a large solubility of CO₂ in micelles can be attributed to the affinity of CO₂ with the fluorinated chain tail of CO₂-philic surfactant *N*-EtFOSA,^[12,14] as well as the stable *N*-EtFOSA micelles formed in the IL, which is favorable to accommodating more CO₂ molecules inside.

The microstructure of *N*-EtFOSA/TMGA solution ([*N*-EtFOSA] = 3.0 wt%) in the presence of liquid CO₂ was investigated by high-pressure small-angle X-ray scattering (SAXS). Figure 3A shows the SAXS curves of *N*-EtFOSA/TMGA solution at various pressures of liquid CO₂. In the small-angle region, the scattering intensity decreases with increasing CO₂ pressure, which may be caused both by the decreased micellar size and the changed difference in electron densities between the surfactant and solvent by the dissolution of CO₂.^[15] The generalized indirect Fourier transformation (GIFT) gives the pair distance distribution function, $p(r)$, which is usually utilized to characterize the basic geometry of the aggregates (such as spherical, cylindrical, planar, etc.) in micellar systems.^[16] As shown in the inset of Figure 3A, the $p(r)$ curves are bell-shaped, indicating that the micelles are spherical.^[16] The micelle size calculated from distance distribution function at different pressures is plotted as the function of R_{CO_2} (Figure 3B). The micellar size increases

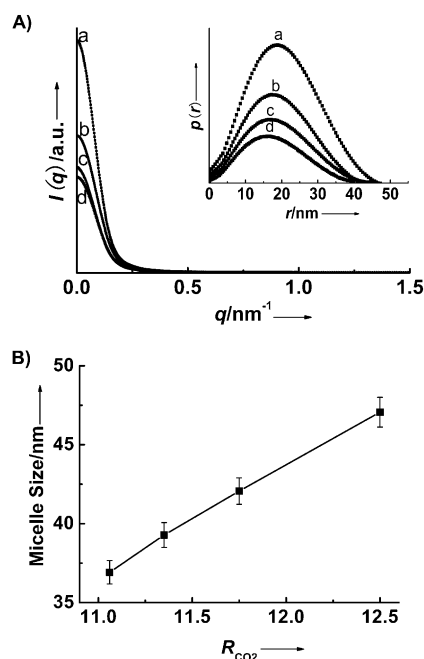


Figure 3. SAXS curves (A) and distance distribution function ($p(r)$) curves (inset) of *N*-EtFOSA/TMGA solution ([*N*-EtFOSA] = 3.0 wt%) at CO₂ pressure of 5.7 MPa (a), 6.5 MPa (b), 7.5 MPa (c), and 8.5 MPa (d). B) Micelle size versus R_{CO_2} .

with the increasing amount of the CO₂ solubilized in the micelles. This is similar to the traditional oil-in-water microemulsions^[17] and CO₂-in-water microemulsions.^[8a] At R_{CO_2} = 12.5, the micelles have an average size of 47 nm, much larger than the CO₂-free micelles. It can be concluded from above results that CO₂-in-IL microemulsions were formed in CO₂/*N*-EtFOSA/TMGA system at these pressures. The CO₂-swollen micelles are “tunable” because their size can be easily tuned by the pressure of CO₂, that is, the amount of solubilized CO₂.

The possibility for the formation of CO₂-in-IL microemulsions was also investigated at other experimental conditions. The microstructures of the *N*-EtFOSA/TMGA solution ([*N*-EtFOSA] = 3.0 wt%) at 0 MPa, 2.0 MPa, 4.0 MPa, and 5.0 MPa were investigated by SAXS analysis. No significant change in the micellar size (22.1 ± 1.1 nm) was observed with increasing pressure of CO₂ (Figure S2). This result indicates that compressed gaseous CO₂ is incapable of swelling the micelles effectively. That is, the CO₂-in-TMGA microemulsion cannot be formed at pressures lower than 5.7 MPa.

Moreover, solubility determination and the SAXS technique showed that CO₂-in-IL microemulsion in CO₂/*N*-EtFOSA/1-octyl-3-methylimidazolium chloride ([omim]Cl) system ([*N*-EtFOSA] = 3.0 wt%) was also formed at CO₂ pressures higher than 5.7 MPa (Figures S3 and S4). In comparison with the CO₂-in-TMGA microemulsion, less CO₂ was solubilized in the micelles of CO₂-in-[omim]Cl microemulsion. This can be attributed to the fact that the micelles formed in TMGA are more stable than those formed in [omim]Cl, owing to the stronger hydrogen-bonding interaction between acetate in TMGA and the NH group of *N*-

EtFOSA than that between Cl^- in [omim]Cl and the NH group of *N*-EtFOSA.^[12b]

Furthermore, we explored the application of CO_2 -in-IL microemulsions in fabrication of metal–organic frameworks (MOFs), which present great potential in gas storage, separation, and catalysis.^[18] Lanthanum–BTC (BTC = benzenetricarboxylate) MOF was synthesized in the CO_2 -in-TMGA microemulsion at various pressures. Figure 4a,b shows the SEM and TEM images of the MOF synthesized at 5.8 MPa. Interestingly, the MOF is porous, and the pore

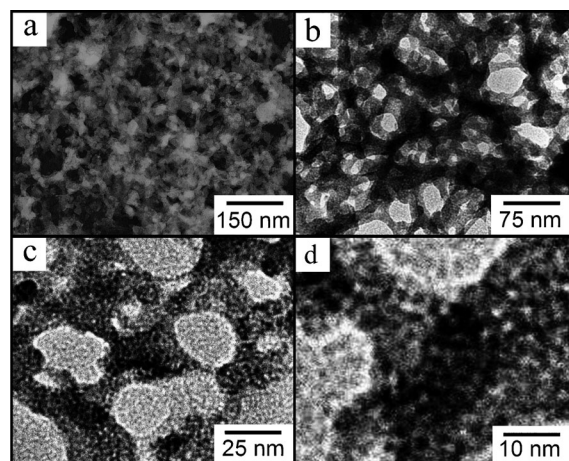
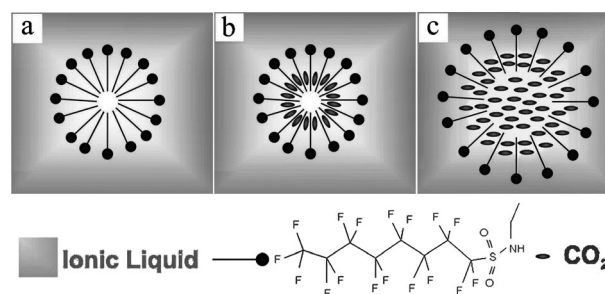


Figure 4. a) SEM image and b–d) TEM images of MOF synthesized in CO_2 -in-TMGA microemulsion at 5.8 MPa.

size is in the range 20–50 nm, which corresponds to the micellar size of the CO_2 -in-IL microemulsions. The main reason for the formation of the pores is that the micelles cannot solubilize the precursors of MOF, $\text{La}(\text{NO}_3)_3$ and H_3BTC , which are dissolved in the continuous phase of the microemulsion. Therefore, the micelles act as the template for the pores of MOF. The magnified TEM images show the formation of small pores in the range 2–3 nm (Figure 4c,d). As discussed above, the MOF is formed in the continuous phase of the microemulsion, which is an IL– CO_2 solution due to the dissolution of CO_2 in the IL. It is well known that the viscosity of ILs is much higher than that of conventional molecular solvents. Thus, some IL– CO_2 solution can be trapped during the formation of the MOF, leaving the smaller pores after the IL and CO_2 are removed. The MOFs with bimodal porous structure were also obtained at other pressures of 7.5 MPa and 10.0 MPa (Figure S5). The powder X-ray diffraction pattern (Figure S6) shows that the MOF is crystalline and all diffraction peaks can be well indexed to a known MOF of $\text{La}(\text{1,3,5-BTC})\cdot 6\text{H}_2\text{O}$.^[19] The existence of the nanosized pores in the MOFs can enhance the mass transfer in the applications such as adsorption, separation, and catalysis.

On the basis of the above results, a scheme for the formation of CO_2 -in-IL microemulsion is illustrated in Scheme 1. In the absence of CO_2 , the surfactant molecules self-aggregate into spherical micelles, by the hydrogen bonding interactions between the IL anions and the NH group of



Scheme 1. Schematic illustration for the formation of CO_2 -in-IL microemulsion: a) “dry” micelle dispersed in IL; b) CO_2 -bound micelle; c) CO_2 -swollen micelle.

N-EtFOSA.^[12b] The hydrophilic head groups of *N*-EtFOSA point to the continuous IL phase, while the fluorinated tails arrange towards the inner, forming the “dry” micelles with the empty cores (Scheme 1a). By taking into account the properties of the IL, the surfactant, and CO_2 , there are mainly three locations for CO_2 to exist in the micellar solution, namely, the IL continuous phase, the surfactant interface, and the apolar micellar cores. At the lower CO_2 pressures, gaseous CO_2 can dissolve in IL continuous phase and can enter surfactant interfacial region because the strong interaction between CO_2 and the fluorinated tails of the surfactant. CO_2 interacting with the surfactant is denoted as “bound CO_2 ”, which is incapable of expanding the micelles (Scheme 1b). As the pressure exceeds the saturated vapor pressure of CO_2 , liquefied CO_2 enters into the micellar cores to form CO_2 domains, and a CO_2 -in-IL microemulsion is formed, and the micelles are expanded (Scheme 1c). Since the CO_2 content can be tuned by pressure, as discussed above, the CO_2 -swollen micelles are thus “tunable” solely by the control of pressure.

In summary, a CO_2 -in-IL microemulsion was created for the first time. The CO_2 -swollen micelles are “tunable” because the micellar size can be easily adjusted by the pressure of CO_2 . This novel kind of microemulsion has potential applications in various fields, such as materials synthesis, chemical reactions, and extraction.

Experimental Section

Materials: The surfactant *N*-EtFOSA (> 95 %) was purchased from Guangzhou Leelchem Corporation. TMGA was synthesized by direct neutralization of 1,1,3,3-tetramethylguanidine with acetic acid. [omim]Cl was purchased from Centre of Green Chemistry and Catalysis, LICP, CAS (purity > 99 %). CO_2 (purity > 99.9 %) was provided by Beijing Analysis Instrument Factory. Lanthanum(III) nitrate hydrate ($\text{La}(\text{NO}_3)_3\cdot 6\text{H}_2\text{O}$) (A.R. grade) was purchased from Sinopharm Chemical Reagent Co., Ltd. 1,3,5-Benzenetricarboxylic acid (H_3BTC) (purity 95 %) was purchased from Aldrich.

Freeze fracture electron microscopy: The sample of *N*-EtFOSA/TMGA solution ([*N*-EtFOSA] = 3.0 wt %) was frozen and clamped under liquid nitrogen inside the vacuum chamber of the freeze-etching apparatus (Balzers/BAL-TE, Liechtenstein), and fractured by a microtome arm. Pt/C was coated immediately on the sample fracture sections to capture the configuration on the surfaces, and the replica was transferred onto copper grids for transmission electron microscopy observation (JeoL-1010).

Determination of CO₂ solubility in pure IL and *N*-EtFOSA/IL solution: In a typical experiment, the desired amount of *N*-EtFOSA/IL solution was loaded into the view cell. The view cell was placed in the constant-temperature water bath. After the thermal equilibrium had been reached, CO₂ was charged into the view cell. The magnetic stirrer was used to accelerate the mixing of CO₂ and the solution. After equilibrium had been reached, the valve of the sample bomb for sampling the liquid phase was opened slowly to collect some sample. At the same time, the volume of the view cell was adjusted to keep the pressure unchanged during the sampling process. The sample bomb was then removed for composition analysis. To analyze the composition of the sample, the mass of the sample bomb was first determined by an electronic balance (Mettler MP1200) with a resolution of 0.001 g. The mass of the sample was known from the masses of the sample bomb with and without the sample. The CO₂ in the sample bomb was then released slowly. The mass of the CO₂ in the sample was easily known from the mass change of the sample bomb before and after releasing CO₂ because the IL and the surfactant are not volatile. The CO₂ solubility was known from the masses of the liquid and the gas in the sample.

High-pressure SAXS experiment: SAXS experiments were carried out at Beamline 4B9A at Beijing Synchrotron Radiation Facility (BSRF). The data were collected using a CCD detector (MAR), which had a maximum resolution of 2048 × 2048 pixels. The wavelength used was 1.53 Å, and the distance of sample to detector was 1.66 m. In a typical experiment, the desired amount of *N*-EtFOSA/IL solution was added into the sample cell. After the system had reached thermal equilibrium, CO₂ was charged into the cell until the desired pressure was reached with stirring. The X-ray scattering data were recorded after enough equilibration time.

Synthesis of MOFs and characterization: La(NO₃)₃·6H₂O (0.15 mmol) and H₃BTC (0.15 mmol) were added into an autoclave containing *N*-EtFOSA/TMGA solution (10 g, [*N*-EtFOSA] = 3.0 wt %). Then, CO₂ was charged into the autoclave until the desired pressure was reached. The solution was stirred at 293.2 K for 24 h. After CO₂ was released, the precipitate was collected by centrifugation, washed several times with ethanol and water, and dried under vacuum at 55 °C. The morphology of the product obtained was characterized by SEM on a HITACHI S-4800 instrument and TEM on a JeoL-1010 instrument operated at 100 kV. Powder XRD analysis of the sample was performed (Model D/MAX2500, Rigaku) with Cu Kα radiation.

Received: June 10, 2011

Published online: September 5, 2011

Keywords: emulsions · ionic liquids · metal-organic frameworks · micelles

- [1] a) X. Nasongkla, H. A. Shuai, B. D. Weinberg, J. Pink, D. A. Boothman, J. M. Gao, *Angew. Chem.* **2004**, *116*, 6483; *Angew. Chem. Int. Ed.* **2004**, *43*, 6323; b) Y. Lee, T. Ishii, H. Cabral, H. J. Kim, J. H. Seo, N. Nishiyama, H. Oshima, K. Osada, K. Kataoka, *Angew. Chem.* **2009**, *121*, 5413; *Angew. Chem. Int. Ed.* **2009**, *48*, 5309.
- [2] a) J. P. K. Tan, S. H. Kim, F. Nederberg, E. A. Appel, R. M. Waymouth, Y. Zhang, J. L. Hedrick, Y. Y. Yang, *Small* **2009**, *5*, 1504; b) R. L. Shinde, A. B. Jindal, P. V. Devarajan, *Curr. Nanosci.* **2011**, *7*, 119.
- [3] a) R. N. Mitra, A. Dasgupta, D. Das, S. Roy, S. Debnath, P. K. Das, *Langmuir* **2005**, *21*, 12115; b) G. P. Zhang, H. H. Zhou, J. Q. Hu, M. Liu, Y. F. Kuang, *Green Chem.* **2009**, *11*, 1428; c) D. Meltzer, D. Avnir, M. Fanun, V. Gutkin, I. Popov, R. Schoenmaeker, M. Schwarze, J. Blum, *J. Mol. Catal. A* **2011**, *335*, 8.
- [4] a) B. A. Simmons, S. C. Li, V. T. John, G. L. McPherson, A. Bose, W. L. Zhou, J. B. He, *Nano Lett.* **2002**, *2*, 263; b) M. A. Hillmyer, *Science* **2007**, *317*, 604; c) M. F. Wang, S. Kumar, A. Lee, N. Felorzabih, L. Shen, F. Zhao, P. Froimowicz, G. D. Scholes, M. A. Winnik, *J. Am. Chem. Soc.* **2008**, *130*, 9481.
- [5] a) C. A. Eckert, B. L. Knutson, P. G. Debenedetti, *Nature* **1996**, *383*, 313; b) E. J. Beckman, *Science* **1996**, *271*, 613; c) G. B. Jacobson, C. T. Lee, K. P. Johnston, W. Tumas, *J. Am. Chem. Soc.* **1999**, *121*, 11902; d) P. Raveendran, Y. Ikushima, S. L. Wallen, *Acc. Chem. Res.* **2005**, *38*, 478; e) P. G. Jessop, B. Subramaniam, *Chem. Rev.* **2007**, *107*, 2666; f) Q. L. Chen, E. J. Beckman, *Green Chem.* **2008**, *10*, 934; g) J. W. Ford, M. E. Janakat, J. Lu, C. L. Liotta, C. A. Eckert, *J. Org. Chem.* **2008**, *73*, 3364.
- [6] a) M. Smiglak, A. Metlen, R. D. Rogers, *Acc. Chem. Res.* **2007**, *40*, 1182; b) D. Chaturvedi, *Curr. Org. Chem.* **2011**, *15*, 1236; c) C. D. Hubbard, P. Illner, R. van Eldik, *Chem. Soc. Rev.* **2011**, *40*, 272; d) M. Petkovic, K. R. Seddon, L. P. N. Rebelo, C. S. Pereira, S. Cristina, *Chem. Soc. Rev.* **2011**, *40*, 1383.
- [7] a) K. P. Johnston, K. L. Harrison, M. J. Clarke, S. M. Howdle, M. P. Heitz, F. V. Bright, C. Carlier, T. W. Randolph, *Science* **1996**, *271*, 624; b) J. Eastoe, S. Gold, S. Rogers, P. Wyatt, D. C. Steytler, A. Gurgel, R. K. Heenan, X. Fan, E. J. Beckman, R. M. Enick, *Angew. Chem.* **2006**, *118*, 3757; *Angew. Chem. Int. Ed.* **2006**, *45*, 3675; c) Y. Takebayashi, M. Sagisaka, K. Sue, S. Yoda, Y. Hakuta, T. Furuya, *J. Phys. Chem. B* **2011**, *115*, 6111; d) M. Sagisaka, S. Iwama, S. Hasegawa, A. Yoshizawa, A. Mohamed, S. Cummings, S. E. Rogers, R. K. Heenan, J. Eastoe, *Langmuir* **2011**, *27*, 5772.
- [8] a) C. T. Lee, W. Ryoo, P. G. Smith, J. Arellano, D. R. Mitchell, R. J. Lagow, S. E. Webber, K. P. Johnston, *J. Am. Chem. Soc.* **2003**, *125*, 3181; b) M. Schwan, L. G. A. Kramer, T. Sottmann, R. Strey, *Phys. Chem. Chem. Phys.* **2010**, *12*, 6247.
- [9] a) H. X. Gao, J. C. Li, B. X. Han, W. N. Chen, J. L. Zhang, R. Zhang, D. D. Yan, *Phys. Chem. Chem. Phys.* **2004**, *6*, 2914; b) J. Eastoe, S. Gold, S. E. Rogers, A. Paul, T. Welton, R. K. Heenan, I. Grillo, *J. Am. Chem. Soc.* **2005**, *127*, 7302; c) A. Adhikari, D. K. Das, D. K. Sasmal, K. Bhattacharyya, *J. Phys. Chem. A* **2009**, *113*, 3737; d) F. Gayet, C. E. Kalamouni, P. Lavedan, J. D. Marty, A. Brûlet, N. L. Viguerie, *Langmuir* **2009**, *25*, 9741; e) R. Pramanik, S. Sarkar, C. Ghatak, V. G. Rao, P. Setua, N. Sarkar, *J. Phys. Chem. B* **2010**, *114*, 7579; f) H. H. Lu, X. Q. An, W. G. Shen, *J. Chem. Eng. Data* **2011**, *56*, 502.
- [10] a) Y. A. Gao, S. B. Han, B. X. Han, G. Z. Li, D. Shen, Z. H. Li, J. M. Du, W. G. Hou, G. Y. Zhang, *Langmuir* **2005**, *21*, 5681; b) Z. N. Wang, F. Liu, Y. A. Gao, W. C. Zhuang, L. M. Xu, B. X. Han, G. Z. Li, G. Y. Zhang, *Langmuir* **2005**, *21*, 4931; c) Y. A. Gao, N. Li, L. Q. Zheng, X. Y. Zhao, S. H. Zhang, B. X. Han, W. G. Hou, G. Z. Li, *Green Chem.* **2006**, *8*, 43; d) D. Seth, A. Chakraborty, P. Setua, N. Sarkar, *J. Chem. Phys.* **2007**, *126*, 224512; e) M. M. Zaman, N. Kamiya, K. Nakashima, M. Goto, *ChemPhysChem* **2008**, *9*, 689; f) H. X. Wu, H. X. Wang, L. Xue, X. Y. Li, *J. Colloid Interface Sci.* **2011**, *353*, 476.
- [11] S. Q. Cheng, J. L. Zhang, Z. F. Zhang, B. X. Han, *Chem. Commun.* **2007**, *24*, 2497.
- [12] a) J. H. Liu, S. Q. Cheng, J. L. Zhang, X. Y. Feng, X. G. Fu, B. X. Han, *Angew. Chem.* **2007**, *119*, 3377; *Angew. Chem. Int. Ed.* **2007**, *46*, 3313; b) A. Chandran, K. Prakash, S. Senapati, *J. Am. Chem. Soc.* **2010**, *132*, 12511.
- [13] a) L. Y. Wang, X. Chen, Y. C. Chai, J. C. Hao, Z. M. Sui, W. C. Zhuang, Z. M. Sun, *Chem. Commun.* **2004**, 2840; b) J. Hao, T. Zemb, *Curr. Opin. Colloid Interface Sci.* **2007**, *12*, 129; c) T. L. Greaves, C. J. Drummond, *Chem. Soc. Rev.* **2008**, *37*, 1709; d) N. Li, S. H. Zhang, L. Q. Zheng, T. Inoue, *Langmuir* **2009**, *25*, 10473.
- [14] Y. J. Zhao, J. L. Zhang, B. X. Han, J. L. Song, J. S. Li, Q. Wang, *Angew. Chem.* **2011**, *123*, 662; *Angew. Chem. Int. Ed.* **2011**, *50*, 636.
- [15] J. L. Zhang, B. X. Han, J. C. Liu, X. G. Zhang, G. Y. Yang, J. He, Z. M. Liu, T. Jiang, *J. Chem. Phys.* **2003**, *118*, 3329.

- [16] a) L. K. Shrestha, O. Glatter, K. Aramaki, *J. Phys. Chem. B* **2009**, *113*, 6290; b) L. K. Shrestha, R. G. Shrestha, D. Varade, K. Aramaki, *Langmuir* **2009**, *25*, 4435; c) Y. J. Zhao, J. L. Zhang, Q. Wang, W. Li, J. S. Li, B. X. Han, Z. H. Wu, K. H. Zhang, Z. H. Li, *Langmuir* **2010**, *26*, 4581; d) Y. J. Zhao, J. L. Zhang, Q. Wang, J. S. Li, B. X. Han, *Phys. Chem. Chem. Phys.* **2011**, *13*, 684; e) J. L. Zhang, B. X. Han, Y. J. Zhao, J. S. Li, G. Y. Yang, *Chem. Eur. J.* **2011**, *17*, 4266.
- [17] a) A. Costa, L. Carmen, O. Brino, H. Chaimovich, M. J. Politi, *Langmuir* **1992**, *8*, 2417; b) R. E. Riter, E. P. Undiks, N. E. Levinger, *J. Am. Chem. Soc.* **1998**, *120*, 6062.
- [18] a) Y. K. Hwang, D. Y. Hong, J. S. Chang, S. H. Jhung, Y. K. Seo, J. Kim, A. Vimont, M. Daturi, C. Serre, G. Ferey, *Angew. Chem.* **2008**, *120*, 4212; *Angew. Chem. Int. Ed.* **2008**, *47*, 4144; b) S. Natarajan, P. Mahata, *Chem. Soc. Rev.* **2009**, *38*, 2304; c) Z. Q. Wang, S. M. Cohen, *Chem. Soc. Rev.* **2009**, *38*, 1315; d) O. K. Farha, J. T. Hupp, *Acc. Chem. Res.* **2010**, *43*, 1166; e) S. T. Meek, J. A. Greathouse, M. D. Allendorf, *Adv. Mater.* **2011**, *23*, 249.
- [19] a) K. Liu, G. Jia, Y. H. Zheng, Y. H. Song, M. Yang, Y. J. Huang, L. H. Zhang, H. You, *Inorg. Chem. Commun.* **2009**, *12*, 1246; b) K. Liu, Y. H. Zheng, G. A. Jia, M. Yang, Y. H. Song, N. Guo, H. P. You, *J. Solid State Chem.* **2010**, *183*, 2309; c) K. Liu, H. P. You, Y. H. Zheng, G. Jia, Y. J. Huang, M. Yang, Y. H. Song, L. H. Zhang, H. J. Zhang, *Cryst. Growth Des.* **2010**, *10*, 16; d) Y. J. Zhao, J. L. Zhang, J. L. Song, J. S. Li, J. L. Liu, T. B. Wu, P. Zhang, B. X. Han, *Green Chem.* **2011**, *13*, 2078.